J Mol Model (2005) 11: 351–361
DOI 10.1007/s00894-005-0267-4

ORIGINAL PAPER

Piotr Kornel Wawrzyniak · Jarosław Panek
Jan Lundell · Zdzisław Latajka

On the nature of bonding in HCOOH...Ar and HCOOH...Kr complexes

Received: 29 October 2004 / Accepted: 31 January 2005 / Published online: 12 May 2005

Abstract The chemical interaction in HCOOH...Ng (Ng = Ar, Kr) complex was analyzed by topological analysis of the electron density based on Atoms-In-Molecules theory. For all computationally stable equilibrium structures of 1:1 HCOOH...Ng complexes, an intermolecular bond path with a "bond" critical point was found and perturbation of formic acid (FA) atomic basins and electron density was observed. The intermolecular interaction between the two complex subunits can be classified, according to its nature, as a closed-shell van der Waals type of interaction. However, one of the computed structures (complex II), pictures a noble gas atom attached linearly to the acidic O–H tail of FA. In this particular case, the electron density at the intermolecular bond critical point was found to resemble a hydrogen-bonded system and thus, may be termed a hydrogen-bond-like interaction. This change in the nature of the interaction is also shown by large perturbations of the FA properties found for this complex structure. The structural and vibrational perturbations are larger than for the other three structures and they increase for the Kr complexes compared to the Ar complex.

Keywords Noble gas · Complex · Computational chemistry · Electron density · Formic acid

Introduction

Despite the common use of the matrix isolation technique to investigate entrapped chemical entities in solid-state atomic or molecular matrices, interaction mechanisms between the trapped molecule (guest) and the lattice (host) are not completely understood on the atomic level [1, 2]. Noble gases are widely used as a matrix environment because of their inertness. Thus, it seems that understanding the interactions and the nature of the chemical bonds they can form is a crucial case. In order to gain better insight into what occurs in low-temperature matrices on the molecular level, atomistic and/or large-scale molecular simulations are needed. However, computational simulations may yield reasonable results only if sufficiently high theoretical levels or accurate interaction models are employed. This influences the selection of the model systems and restricts their size, especially in high-level ab initio approaches.

Formic acid (FA), seems to be a good choice for a model system, being the simplest organic acid exhibiting both carbonyl and hydroxyl groups. These functional groups produce attractive interaction sites, which appear as a good model for understanding the interactions of more complicated systems. There are several experimental reports describing the activity of FA and its ability to engage in intermolecular interactions [3–9]. Recently, extensive studies on FA and its molecular dynamics in low-temperature matrices have been performed [6–14], focusing especially on the internal rotation between *trans*-FA and its higher-energy conformer *cis*-FA. Along with IR-induced interconversion, a backward reaction from *cis*- to *trans*-FA was found, which was assigned to a phonon-assisted tunneling mechanism [10, 11]. This process exhibits both temperature and environment dependence. Also, the two conformers of FA isolated in low-temperature matrices were found to show differences in their photo dissociation behavior [12]. All these experimentally observed processes appear to be aware of the surrounding environment, indicating the significance of interactions between the matrix atoms and the FA molecule.

In a recent paper, we discussed the complex between FA and argon [15]. Four stable structures for both *trans*- and *cis*-FA...Ar complexes were reported, of which the

P. K. Wawrzyniak · J. Panek · Z. Latajka
Faculty of Chemistry, University of Wrocław, F. Joliot-Curie 14, 50-383 Wrocław, Poland

J. Lundell (✉)
Chemistry ICT-Center, Department of Chemistry, University of Helsinki, P.O. Box 55, A.I. Virtasen Aukio 1, FIN, 00014 Helsinki, Finland
E-mail: jan.lundell@helsinki.fi
Tel.: +358-9-19150165
Fax: +358-9-19150466

structure type with the argon atom located between carboxylic hydrogen and oxygen was characterized for the first time. The planar geometry, picturing an argon atom interacting with the OH-tail of FA molecule, was found to be the global minimum structure for both conformer complexes. The BSSE-corrected interaction energies computed at the CCSD(T)/6-311 + + G(2d,2p), 6-311 + G(3df)(Ar)//MP2(full)/6-311 + + G(2d, 2p), 6-311 + G(3df)(Ar) level were −1.50 and −2.01 kJ mol^{-1} for the *trans*- and *cis*- complexes, respectively. Comparison of the calculated infrared spectra of the complex and monomer revealed large shifts, especially for the global minimum structure. The OH stretching mode (νOH) appeared red shifted by 4.0 (*cis*) and 8.0 cm^{-1} (*trans*), whereas for the COH torsion (τCOH) mode large blue shift was present: 14.1 (*cis*) and 19.3 cm^{-1} (*trans*). Moreover, it was found that the stretching modes are the most affected by BSSE-correction applied during the optimization of the complex equilibrium structure. The intermolecular stretching frequencies were noted to increase and the intramolecular stretching frequencies to decrease compared to calculations without the BSSE-correction.

Here, we report computational results for *trans*- and *cis*-FA complexed with one krypton atom and compare them with those obtained for the FA...Ar system. The structural parameters, energetics and vibrational properties are investigated, together with the influence of the basis set superposition error (BSSE) on the data obtained. Our main task is to examine the nature of the FA...Ar and FA...Kr chemical bonds under the circumstances of the topological analysis of the electron density, within Atoms-in-Molecules theory. Also, the computational results are used to gain insight into the qualitative FA...Ng chemical properties that can be used to develop analytical potential models for large-scale molecular dynamics simulations.

Computational methods

All the calculations were performed with the Gaussian 03 [16] package of codes. All calculations were performed using second order Møller–Plesset perturbation theory (MP2) [17]. The standard 6-311 + + G(2d,2p) basis set was used for all atoms of FA and the 6-311 + G(3df) basis set was used for argon and krypton. An all-electron treatment was used in the calculations. All the frequencies were calculated analytically within the harmonic approximation for both the FA monomer and the FA...Ng complexes.

The computed interaction energies were evaluated as the difference between the complex and the monomers at infinite distance, where the monomer wave function was derived in the complex-centered basis set. This procedure corresponds to the counterpoise correction (CP) proposed by Boys and Bernardi [18], aimed at minimizing the BSSE [19] in the interaction energy. The interaction energies were also estimated at higher order perturbation theory (up to MP4(SDQ)) and with the coupled cluster method (up to CCSD(T)), using the MP2-optimized equilibrium structures. The BSSE-corrected structure optimizations were performed and the BSSE-corrected frequencies were computed according to the method proposed by Simon et al. [20], as implemented in the GAUSSIAN program.

Topological analysis of electron density within AIM theory [21, 22] was performed with the AIMPAC package developed by Biegler–Koenig et al. [23]. As required by AIMPAC codes, the wave functions for these analyses were obtained from MP2 calculations, when 6d-component and 10f-component functions in their Cartesian form were used.

Results and discussion

Equilibrium structures of FA...Kr

Computationally, four equilibrium structures, illustrated in Fig. 1, were found for the FA...Kr complex. The intermolecular structures are similar to those described earlier for complexes where FA interacts with argon [15]. Structures II, III and IV represent planar complexes, while geometry I shows a Kr atom lying above the FA molecular plane. This structure lowers the symmetry upon complexation, in contrast to the three other structures, which preserve the FA symmetry elements and the C_s symmetry group. The interaction in complex I results in the deformation of the planarity of the FA, which is nominally bent out from the molecular plane. The computed structural parameters for each complex structure are shown in Table 1.

The computed BSSE-corrected interaction energies are collected in Table 2. The computed energies at every computational level indicate krypton to form more stable complexes, as expected based on the higher static polarizability of the Ng atom. The computed interaction are between −0.6 and −1.8 kJ mol^{-1}, depending of the complex structure and the computational level used. Moreover, the intermolecular potential energy surface of the FA...Kr complex is very flat and the Kr atom can sample large areas of the intermolecular space. In the case of argon complexes [15] this flatness was connected with the fact that the noble gas atom is found to exhibit a thermally averaged structure in microwave experiment [24] instead of a local complex structure found computationally.

The computed vibrational spectra of *trans*- and *cis*-FA upon complexation with a krypton atom are collected in Table 3. The complex structures I, III and IV possess similar FA subunit spectra to the unperturbed monomer. The most profound perturbation is found for the CH stretching mode (ca 4 cm^{-1}) in structures III and IV. The largest shift among all, as one might expect, is found for the lowest energy structure II, featuring the OH...Kr interaction. The OH stretching mode is shifted downwards by 16.8 and 13.9 cm^{-1} for *trans*- and

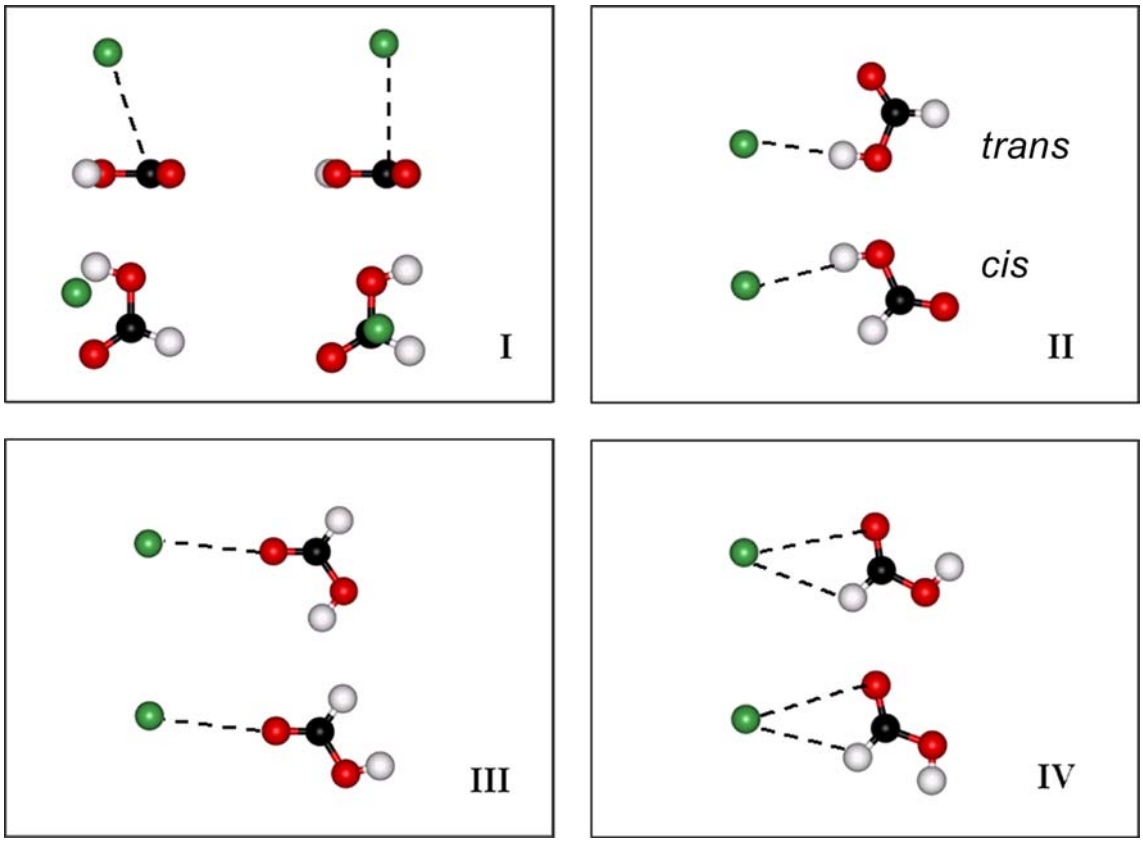

Fig. 1 Computed structures of the *trans*- and *cis*-conformers of the HCOOH...Kr complexes

cis- complexes, respectively. Although the shift is smaller for the latter isomer, it is three and a half times as high as for corresponding Ar complex, while for *trans*-isomer the shift found for Ar is only doubled [25]. Similar changes govern the intensity, which grows from the about 83–191 km mol^{-1} for *trans*- and 185 km mol^{-1} for *cis*-FA...Kr, respectively. Since the OH-tail of FA is involved in the interaction, the skeletal COH modes are also heavily perturbed. Especially the torsional mode is influenced and the computed frequency is blue shifted by 19.4 (*trans*-) and 20.7 cm^{-1} (*cis*-complex) and the intensities decrease by 23 and 27%, respectively.

The structural parameters and vibrational frequencies of complex structure II derived from the BSSE-corrected calculations are collected in Table 4 and compared with the uncorrected results. The BSSE-correction has been noted earlier to affect strongly the computed potential energy surfaces of noble-gas-containing complexes [26, 27]. Therefore, BSSE-accounting optimizations were carried out here for the most stable complex structure to study the effects in the FA...Kr complex. Upon inclusion of BSSE, significant changes are found only for intermolecular parameters, especially for the Kr...H–O distance, which is elongated by 0.17 and 0.14 Å for *trans*- and *cis*-FA...Kr by the BSSE-correction, respectively. This finding agrees with that of Simon and co-workers [20] that counterpoise procedure always leads to reduction of the overestimated BSSE-uncorrected interaction energy and thus, to lengthening the intermolecular bonds. Here, the difference between the corrected and uncorrected complexation energies is about 0.2 kJ mol^{-1}. However, it is noticeable that BSSE introduces a smaller error for complex formed with Kr than with Ar, which agrees with the well-known implication that the basis set superposition error affects mainly intramolecular properties of weakly-bound systems, such as hydrogen bonds and van der Waals complexes. Since the interaction is slightly stronger for FA...Kr, the corrected structures differ less from the uncorrected ones.

For the hydrogen-bonded systems, it was found that applying the counterpoise optimization procedure also affects the vibrational properties of the complex by decreasing the hydrogen bonding stretching frequencies and increasing some of the intermolecular vibrations [20]. Here the interaction is governed by dipole-induced dipole interactions and clearly does not follow the one reported for typical hydrogen-bonded complexes. For HCOOH...Kr (II) complexes, BSSE affects mostly the OH-stretching vibration as well the torsional and intermolecular vibrational modes. The last ones are, in fact, expected to be perturbed since the computed intermolecular distance decreases heavily when BSSE is included in the optimization procedure. It must also be noted that the shifts observed for the intramolecular modes of FA rival those found upon complexation. It seems that BSSE has a crucial effect on the computed vibrational

Table 1 Computed structural parameters[a] of *trans*- and *cis*-HCOOH...Kr at the MP2(full)/6-311 + + G(2d,2p),6-311 + G(3df)(Kr)

	Monomer	I	II	III	IV
trans-HCOOH...Kr					
r(C–O)	1.3480	1.3480	1.3477	1.3480	1.3482
r(C = O)	1.2041	1.2042	1.2044	1.2043	1.2041
r(O–H)	0.9666	0.9668	0.9674	0.9667	0.9667
r(C–H)	1.0899	1.0897	1.0898	1.0896	1.0897
r(Kr–C)		3.8531			
r(Kr–H (OH))			2.7591		
r(Kr–O (CHO))				3.5100	
r(Kr–H (CHO))					3.2305
α(C–O–H)	106.83	106.74	106.80	106.76	106.78
α(O–C = O)	125.08	125.04	125.08	125.05	125.08
α(H–C = O)	125.15	125.15	125.09	125.15	125.10
α(Kr–C–O)		75.89			
α(Kr–H–O)			178.15		
α(Kr–O = C)				176.92	
α(Kr–H–C)					114.14
τ(H–O–C = O)	0.0	−0.2	0.0	0.0	0.0
τ(H–O–C–H)	180.0	179.8	180.0	180.0	180.0
τ(Kr–C–O–H)		62.1			
cis-HCOOH...Kr					
r(C–O)	1.3552	1.3552	1.3542	1.3548	1.3552
r(C = O)	1.1974	1.1975	1.1979	1.1976	1.1975
r(O–H)	0.9616	0.9617	0.9622	0.9617	0.9617
r(C–H)	1.0964	1.0960	1.0963	1.0961	1.0961
r(Kr–C)		3.5978			
r(Kr–H (OH))			2.7488		
r(Kr–O (CHO))				3.4946	
r(Kr–H (CHO))					3.2140
α(C–O–H)	108.90	108.86	108.69	108.96	108.89
α(O–C = O)	122.45	122.40	122.59	122.43	122.44
α(H–C = O)	124.06	124.07	123.98	124.02	123.99
α(Kr–C–O)		87.95			
α(Kr–H–O)			169.43		
α(Kr–O = C)				173.94	
α(Kr–H–C)					114.68
τ(H–O–C = O)	180.0	179.4	180.0	180.0	180.0
τ(H–O–C–H)	0.0	−0.6	0.0	0.0	0.0
τ(Kr–C–O–H)		81.6			

[a] Bond lengths are in Å and angles in degrees.

shifts, especially for weakly bound systems like those in this study. However, more systematic studies of the BSSE-effect on the properties of van der Waals complexes are needed to make more elusive conclusions.

Table 2 Computed BSSE-corrected interaction energies (in kJ mol^{-1}) for *trans*- and *cis*-HCOOH...Kr

	I	II	III	IV
trans-HCOOH...Kr				
MP2//MP2	−1.753	−1.883	−1.264	−1.511
MP3//MP2	−0.941	−1.267	−0.681	−0.959
MP4D//MP2	−1.000	−1.237	−0.772	−0.981
MP4DQ//MP2	−0.759	−0.900	−0.648	−0.757
MP4SDQ//MP2	−0.885	−1.040	−0.736	−0.855
CCSD//MP2	−0.860	−1.028	−0.679	−0.827
CCSD(T)//MP2	−1.385	−1.654	−0.988	−1.284
cis-HCOOH...Kr				
MP2//MP2	−1.820	−2.476	−1.341	−1.629
MP3//MP2	−0.906	−1.905	−0.753	−1.073
MP4D//MP2	−0.954	−1.869	−0.833	−1.089
MP4DQ//MP2	−0.734	−1.534	−0.708	−0.857
MP4SDQ//MP2	−0.868	−1.662	−0.794	−0.965
CCSD//MP2	−0.835	−1.643	−0.741	−0.934
CCSD(T)//MP2	−1.367	−2.271	−1.051	−1.406

AIM results on the FA...Ar and FA...Kr complexes

The existence of a bond path connecting two nuclear attractors (i.e., two nuclei) and a bond critical point in between meets the necessary and sufficient conditions to consider two atoms as being bonded to one another [21]. The AIM study on the FA...Ar and FA...Kr complexes revealed the existence of such a condition for all complex structures considered. The bond-path topologies and electron-density contours for structures II–IV of the complex are shown in Figs. 2 and 3 and they appear to be qualitatively the same for both FA conformer complexes. However, no useful picture could be drawn for the non-planar structure I due to a very complicated electron density situation.

An interesting finding is that Ar and Kr can "bind" in these complexes with elements whose electro negativities are both high (O) and low (H, C), as has been suggested earlier for argon by Bone and Bader [25] However, when forming a complex with FA, the noble gas atom is involved with close contact simultaneously to both oxygen and hydrogen, as found for structure IV. The weak C–H...Ng interaction manifests itself by an increasing bond path curvature near the hydrogen atom. The bond path

Table 3 Computed harmonic vibrational frequencies (in cm^{-1}) and infrared intensities (in km mol^{-1}) of HCOOH...Kr

Assignment[a]	Monomers		I		II		III		IV	
	Freq.	Intens.	Freq.	Intens.	Freq.	Intens.	Freq.	Intens.	Freq.	Intens.
trans-FA										
ν_{OH}	3,784.7	82.7	3,781.9	72.8	3,767.9	191.2	3,782.9	79.2	3,783.4	86.5
ν_{CH}	3,130.9	33.5	3,132.7	32.2	3,131.5	40.8	3,134.9	34.2	3,134.4	32.1
$\nu_{C=O}$	1,788.3	335.8	1,787.3	302.8	1,786.2	301.8	1,787.8	367.9	1,787.7	320.7
γ_{CH}	1,427.1	1.5	1,426.4	1.4	1,427.6	2.5	1,426.5	1.5	1,427.3	1.7
CO–COH def.	1,316.6	9.6	1,317.3	9.7	1,321.0	14.5	1,317.0	9.6	1,317.2	11.6
COH–CO def.	1,124.2	283.4	1,123.9	261.4	1,126.6	262.0	1,124.6	290.9	1,123.8	312.2
ω_{OH}	1,066.3	3.8	1,065.3	4.2	1,065.8	3.3	1,066.6	3.6	1,065.6	3.1
τ_{COH}	676.0	144.0	676.2	174.9	695.4	110.9	677.1	139.5	676.6	139.5
δ_{OCO}	631.7	39.5	632.0	38.0	633.7	35.8	632.6	39.6	632.0	43.6
Inter-molecular modes			41.4	0.7	48.0	2.4	39.7	1.0	41.2	2.1
			33.3	1.7	47.6	0.9	37.9	0.3	37.8	0.4
			23.2	0.0	21.5	1.6	21.9	1.1	25.4	0.1
cis-FA										
ν_{OH}	3,851.2	82.6	3,849.3	78.3	3,837.3	185.3	3,850.2	87.0	3,850.5	84.2
ν_{CH}	3,042.9	64.7	3,046.7	57.7	3,044.3	64.6	3,047.0	65.6	3,046.9	60.7
$\nu_{C=O}$	1,828.5	269.2	1,828.4	244.9	1,826.6	306.7	1,827.9	298.2	1,828.2	252.0
γ_{CH}	1,442.4	0.1	1,441.2	0.1	1,442.0	0.7	1,442.0	0.0	1,442.6	0.9
CO–COH def.	1,287.3	297.3	1,287.2	277.6	1,295.0	245.8	1,286.8	307.8	1,286.9	320.4
COH–CO def.	1,113.4	79.2	1,113.2	70.9	1,117.9	92.9	1,114.7	79.4	1,113.6	92.7
ω_{OH}	1,043.7	0.2	1,042.6	0.0	1,043.5	0.1	1,044.2	0.2	1,043.2	0.1
δ_{OCO}	661.2	11.7	661.3	10.7	662.9	7.9	662.4	12.4	661.6	10.6
τ_{COH}	536.8	88.7	533.2	99.5	557.5	65.0	538.6	87.4	537.3	87.3
Inter-molecular modes			62.5	48.0	50.0	3.9	39.0	49.3	42.7	14.0
			38.5	0.7	43.4	51.5	38.5	1.2	39.0	1.1
			16.1	255	19.2	6.6	22.6	10.3	27.8	36.5

[a] ν: stretching, δ: bending, γ: rocking, ω: wagging, τ: torsion, def.: deformation. Assignment of vibrational modes corresponds to the monomer assignment given in [28].

Table 4 Effect of basis set superposition error on equilibrium structures and vibrational frequencies of structure II for *trans*- and *cis*-HCOOH...Kr

	trans-HCOOH...Kr (II)		*cis*-HCOOH...Kr (II)	
	$\chi_{BSSE\text{-}corr.}$	$\Delta\,\chi_{corr.\text{-}uncorr.}$	$\chi_{BSSE\text{-}corr.}$	$\Delta\,\chi_{corr.\text{-}uncorr}$
r(C–O)(Å)	1.3479	0.0002	1.3544	0.0002
r(C=O)(Å)	1.2042	−0.0002	1.1978	−0.0001
r(O–H)(Å)	0.9671	−0.0003	0.9622	0.0000
r(C–H)(Å)	1.0897	−0.0001	1.0961	−0.0002
r(Kr–H)(Å)	2.9333	0.1742	2.8905	0.1417
α(CO–H) (deg.)	106.84	0.04	108.82	0.13
α(O–C=O) (deg.)	125.10	0.02	122.54	−0.05
α(H–C=O) (deg.)	125.10	0.01	123.98	0.00
α(Kr–H–O) (deg.)	179.07	0.92	169.88	0.45
ν_{OH}	3,773.6	5.7	3,840.2	2.9
ν_{CH}	3,132.1	0.6	3,045.7	1.4
$\nu_{C=O}$	1,787.4	1.2	1,826.8	0.2
γ_{CH}	1,427.4	−0.2	1,441.8	−0.2
CO–COH def.	1,319.0	−2.0	1,292.6	−2.4
COH–CO def.	1,125.2	1.4	1,116.7	−1.2
ω_{OH}	1,065.8	0.0	1,043.5	0.0
τ_{COH}	682.7	−12.7	550.8	−6.7
δ_{OCO}	632.6	−1.1	662.4	−0.5
Inter-molecular modes	36.8	−11.2	41.8	−8.2
	31.0	−16.6	34.2	−9.2
	17.2	−4.3	17.9	−1.3

is longer by $\approx 10^{-1}$ than the geometrical distance between the atoms, while for covalent bonds in FA the difference is only $\approx 10^{-4}$.

The electron density of FA is perturbed most for structure II, where the noble gas atom interacting strongly with acidic hydrogen, penetrates the electron cloud of FA quite significantly. This also produces additional disorder in the remaining part of FA, which is especially visible in the deformation of the atomic basins. The complex geometry III exhibits the smallest perturbation of the basins among all the structures, in agreement with small vibrational shifts and insignificant

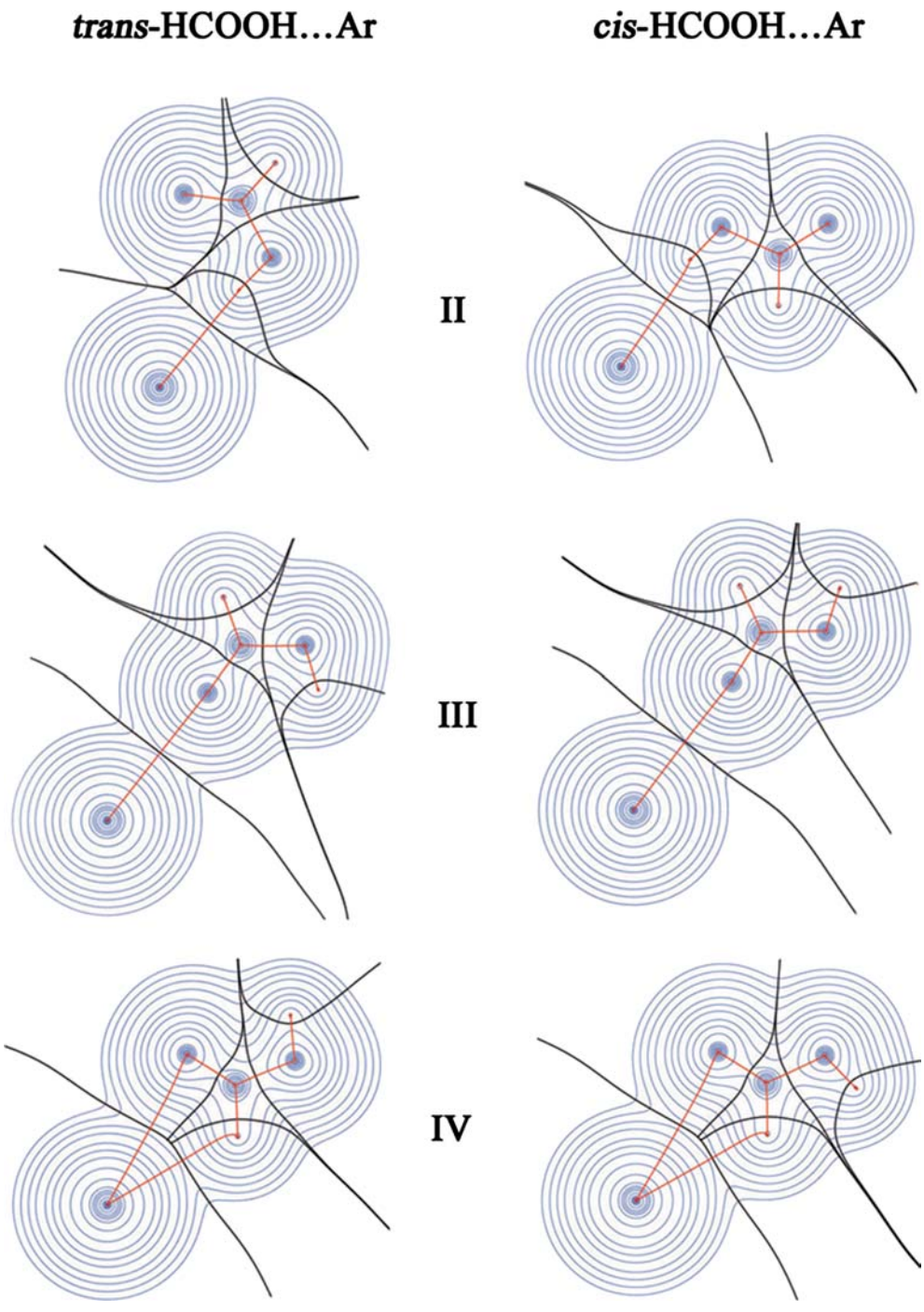

Fig. 2 The bond path topology and electron density contour for *trans*- and *cis*-HCOOH...Ar. The atomic basins are marked in *black*, the bond paths in *red* and electron density in *blue*

changes in the molecular structure of the FA subunit. Nevertheless, the noble gas atom does share space with carbonyl oxygen and penetrates its electron density.

Unlike the three structures described above, structure I reveals a clear difference between *trans*- and *cis*-complexes. In the latter case, both argon and krypton are involved in interactions with the carbon atom, as indicated by the existence of only one intermolecular bond critical point. However, in the *trans*- complex the complexed atom is bound rather to the two oxygens. The noble gas atom situated above the FA molecular plane affects all the atomic basins beneath and leads to a non-planar FA, as seen in the values given in Table 1.

As may be seen in Figs. 4 and 5 picturing the Laplacian of the electron density, the intramolecular bonds of FA are of the shared (i.e., covalent) type and are characterized by a local concentration of the electron density. On the contrary, a positive value of the Laplacian around intermolecular bonds indicates that the density is locally depleted there. However, to be able to

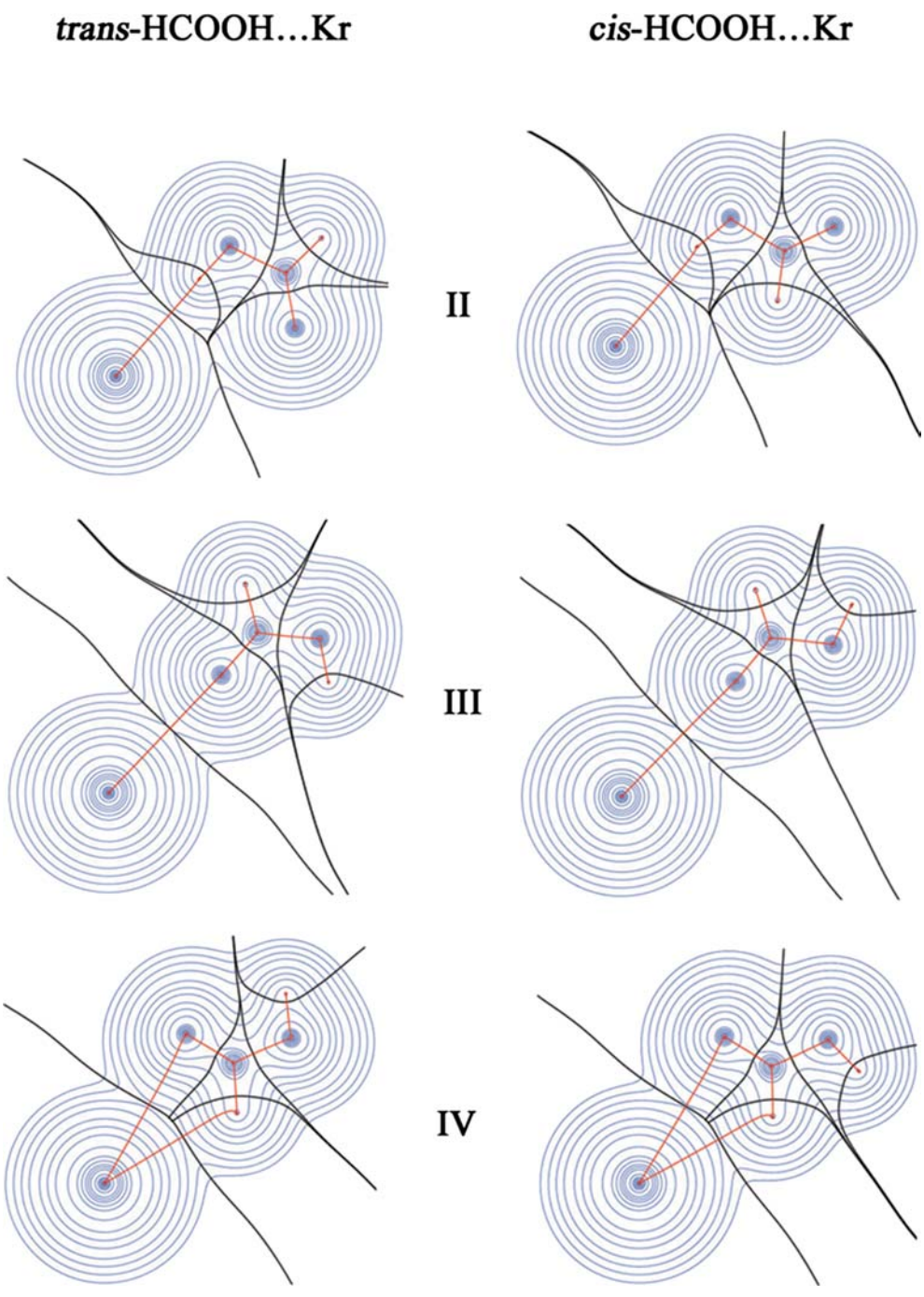

Fig. 3 The bond path topology and electron density contour for *trans*- and *cis*-HCOOH...Kr. The atomic basins are marked in *black*, the bond paths in *red* and electron density in *blue*

discuss precisely the nature of the FA...Ng interaction, the values of electron density and its Laplacian, collected in Tables 5 and 6 must be examined.

Analyzing intermolecular bonding interaction in van der Waals molecules, Bone and Bader stated the existence of van der Waals bonds, which are true counterparts of hydrogen bonds but between pairs of heavy atoms [25]. Indeed, this is the case observed for the FA...Ng complex, as the electron density is around $\approx 10^{-3}$, while its Laplacian possesses small positive value. However, the structure II seems to be somehow special. The Laplacian at the intermolecular bond critical point is almost twice as high as for the other structures. The same applies to the electron density, which is now close to the characteristic value of hydrogen-bonded systems ($\rho \approx 10^{-2}$). This value grows as much as $\approx$10% for *cis*- complex II when Ar is substituted by Kr and at the same time a decrease of the Laplacian is observed. This suggests that the nature of the FA...Ng interaction changes from closed-shell van der Waals type of interaction into more hydrogen-bond-like chemical interaction. The observed change in the Laplacian can be rationalized as follows. For a covalent bond, the Laplacian shows a negative value, whereas for

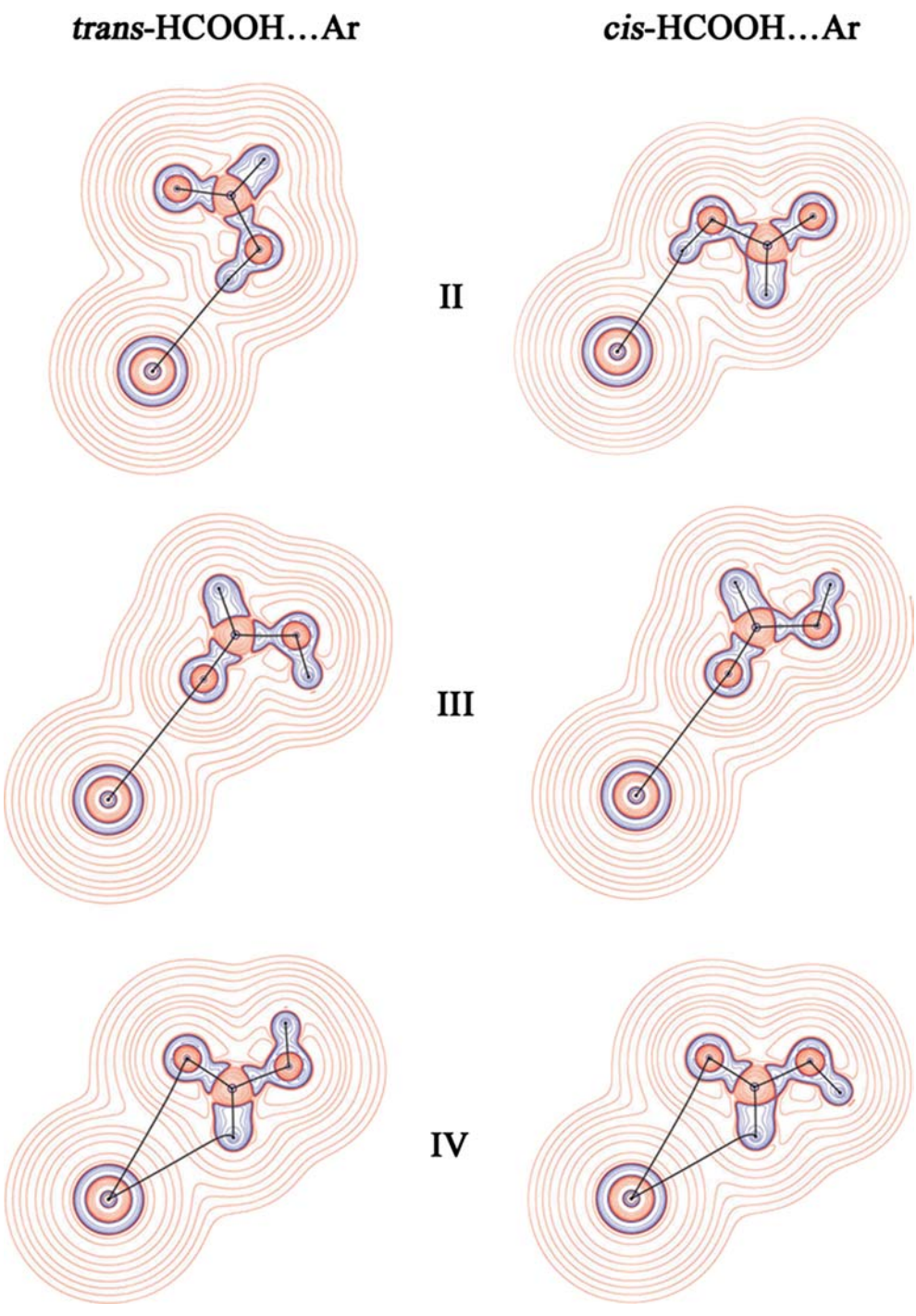

Fig. 4 Laplacian of the electron density for *trans*- and *cis*-HCOOH...Ar. Negative values of Laplacian are marked in *blue*, positive in *red*, the bond paths are colored in *black*

a pure van der Waals complex the value appears to be slightly positive. Going from Ar to Kr complexes and observing a decreasing Laplacian indicates an increase in the electron density. The transformation rationalizes the higher interaction energy for the FA...Kr complex as well as larger shifts in the infrared spectra and stronger perturbation in the structure. Additionally, the intermolecular bond path is observed to decrease in length, especially for the interaction formed with carbonyl hydrogen because these bond paths are curved the most.

Generally, the Kr complexes reveal larger electron densities at the intermolecular bond critical point than the corresponding FA...Ar complexes. However, the nuclear attractor of Kr found in the *trans*-complex I, is translated topologically towards the OH group and thus its relative position differs from that of Ar. This suggests that the interaction is concentrated mainly on the hydroxyl oxygen and in consequence, ρ is smaller at the Kr–O (CHO) bond critical point than for the analogous BCP in the Ar complex.

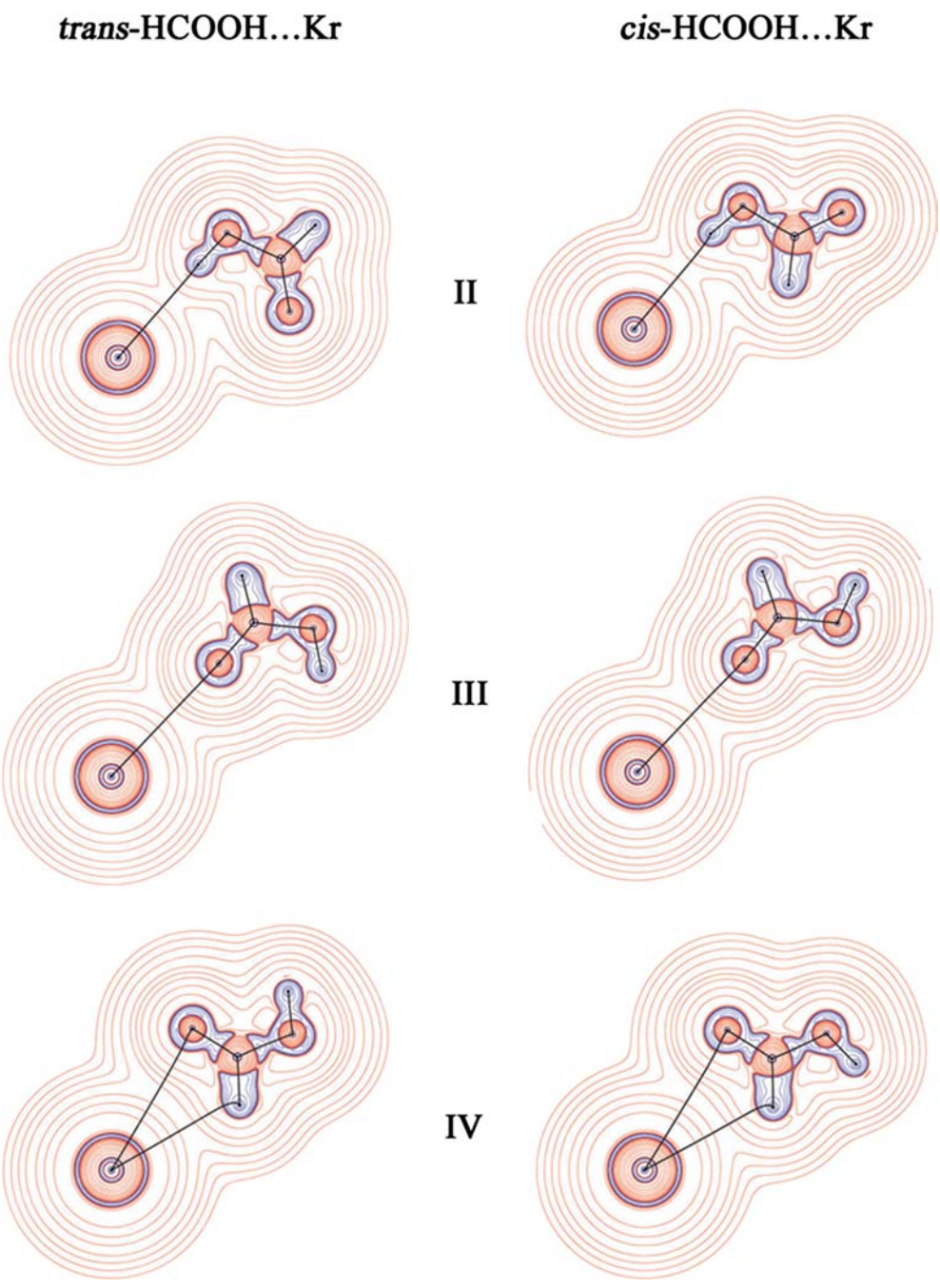

Fig. 5 Laplacian of the electron density for *trans*- and *cis*-HCOOH...Kr. Negative values of Laplacian are marked in *blue*, positive in *red*, the bond paths are colored in *black*

The electron density evaluated for the FA intramolecular bonds is hardly affected at all by the complexation. Although the changes for the Kr-complex are slightly larger than for FA...Ar, they remain insignificant, being three orders of magnitude lower than the value of electron density. However, lowering of the density upon complexation can be seen for C–O and C = O bond critical points for all the complex structures. The high negative charge on the oxygens and electron-rich bonds act as a reservoir of electrons, which may be then distributed over the molecule when a complex is formed. This flow of the electrons, revealed in changes of the dipole moment, confirms the electron density rearrangement.

Conclusions

In the formation of the FA...Ng complex (Ng = Ar, Kr), the main and crucial role seems to be played by the dipole moment of FA. It polarizes the noble gas atom and induces an effective, although small, charge on it. The FA...Ng interaction is dominated by the dipole-induced dipole and dispersion interactions. Thus, the

Table 5 Electron density and its Laplacian at the intermolecular BCP for *trans*- and *cis*-HCOOH...Ar

	BCP	*trans*-FA...Ar	*Cis*-FA...Ar
Electron density (10^{-3})			
Structure I	Ar–C		3.8070
	Ar–O (CHO)	3.4352	
	Ar–O (OH)	3.2276	
Structure II	Ar–H (OH)	6.9882	6.8859
Structure III	Ar–O (CHO)	3.7689	3.9592
Structure IV	Ar–O (CHO)	3.4857	3.5837
	Ar–H (CHO)	3.6316	3.6931
Laplacian (10^{-2})			
Structure I	Ar–C		1.6685
	Ar–O (CHO)	1.4083	
	Ar–O (OH)	1.3684	
Structure II	Ar–H (OH)	2.7997	2.7474
Structure III	Ar–O (CHO)	1.6734	1.7618
Structure IV	Ar–O (CHO)	1.4547	1.4852
	Ar–H (CHO)	1.5514	1.5560

Table 6 Electron density and its Laplacian at the intermolecular BCP for *trans*- and *cis*-HCOOH...Kr

	BCP	*trans*-FA...Kr	*cis*-FA...Kr
Electron density (10^{-3})			
Structure I	Kr–C		3.8474
	Kr–O (CHO)	3.1957	
	Kr–O (OH)	3.2552	
Structure II	Kr–H (OH)	7.1976	7.6142
Structure III	Kr–O (CHO)	4.0798	4.1975
Structure IV	Kr–O (CHO)	3.7993	3.9298
	Kr–H (CHO)	3.6330	3.7759
Laplacian (10^{-2})			
Structure I	Kr–C		1.5660
	Kr–O (CHO)	1.2320	
	Kr–O (OH)	1.2983	
Structure II	Kr–H (OH)	2.5494	2.6898
Structure III	Kr–O (CHO)	1.6890	1.7390
Structure IV	Kr–O (CHO)	1.4724	1.5139
	Kr–H (CHO)	1.4514	1.4821

dipole moment acts as an initial spark in the process of the complex formation and it is clear that the higher the dipole moment the greater dipole it induces on the Ng atom. This explains the larger stability of the *cis*-complexes compared to the *trans*-complexes. On the other hand, the larger polarizability of Kr enhances the interaction compared to Ar complexes. This idea can be extended further to the Xe atom, where the dipole-induced dipole interaction can be expected to be even more significant. Therefore, FA...Xe complexes should be more strongly bonded. Such an effect is clearly visible in the FA/Ng matrix experiments, where the directed FA...Ng interactions affect the FA dynamics.

According to the Atoms-In-Molecules theory, a bond path linking the two complex subunits and the existing well-defined ''bond'' critical point on it indicate a directed interaction for the studied FA...Ar and FA...Kr complexes. Moreover, the atomic basins of FA are strongly perturbed by the noble gas atom and the electron density of FA is noticeably affected as well. This is a major reason leading to a bending of the FA molecule by Ar or Kr located above the molecular plane in structure I in our study.

The bonds binding two monomers can be classified according to their nature as a closed-shell van der Waals type of interaction, with the exception of structure II, where the noble gas atom forms a directed interaction with the OH-tail of FA. The nature of this intermolecular interaction is different from the other complexes studied and, in principle, could be classified as being weak but of hydrogen-bond-type. This explains the large perturbations of the FA molecular properties and extensive shifts in the infrared spectra found for structure II compared with all other computed structures.

The theory of Atoms-In-Molecules seems to produce a reasonable picture of the interaction of FA...Ng (Ng = Ar, Kr) complexes. The computational findings agree with the results obtained from other ab initio studies of this system and provide a quantitative description of the nature of the FA...Ar and FA...Kr chemical interaction to be exploited in large-scale molecular simulations of FA in noble gas matrices.

Acknowledgements WCSS—Wrocław Centre for Networking and Supercomputing is thanked for allocated computational resources. Helsinki University Research Funds and the Academy of Finland are thanked for financial support to JL.

References

1. Apkarian VA, Schwentner N (1999) Chem Rev 99:1481–1514
2. Bondybey VE, Räsänen M, Lammers A (1999) Annu Rep Prog Chem, Sect C: Phys Chem 95:331–372
3. Chang YT, Yamaguchi Y, Miller WH, Schaefer III HF (1987) J Am Chem Soc 109:7245–7253
4. Lundell J, Räsänen M (1993) J Phys Chem 97:9657–9663
5. Lundell J, Räsänen M, Latajka Z (1994) Chem Phys 189:245–260
6. Gantenberg M, Halupka M, Sander W (2000) Chem Eur J 6:1865–1869
7. Priem D, Ha TK, Bauder A (2000) J Chem Phys 113:169–175
8. Robertson WH, Kelley JA, Johnson MA (2000) J Chem Phys 113:7879–7884
9. George L, Sanchez-Garcia E, Sander W (2003) J Phys Chem A 107:6850–6858
10. Pettersson M, Lundell J, Khriachtchev L, Räsänen M (1997) J Am Chem Soc 119:11715–11716
11. Pettersson M, MaÇôas EMS, Khriachtchev L, Lundell J, Fausto R, Räsänen M (2002) J Chem Phys 117:9095–9098
12. Khriachtchev L, MaÇôas E, Pettersson M, Räsänen M (2002) J Am Chem Soc 124:10994–10995
13. Pettersson M, MaÇôas EMS, Khriachtchev L, Fausto R, Räsänen M (2003) J Am Chem Soc 125:4058–4059
14. MaÇôas EMS, Lundell J, Pettersson M, Khriachtchev L, Fausto R, Räsänen M (2003) J Mol Spectrosc 219:70–80
15. Wawrzyniak PK, Panek J, Latajka Z, Lundell J (2004) J Mol Struct 704:297–304
16. Frisch MJ, Trucks GW, Schlegel HB, Scuseria GE, Robb MA, Cheeseman JR, Montgomery Jr JA, Vreven T, Kudin KN, Burant JC, Millam JM, Iyengar SS, Tomasi J, Barone V, Mennucci B, Cossi M, Scalmani G, Rega N, Petersson GA, Nakatsuji H, Hada M, Ehara M, Toyota K, Fukuda R, Hasegawa J, Ishida M, Nakajima T, Honda Y, Kitao O, Nakai H, Klene M, Li X, Knox JE, Hratchian HP, Cross JB, Bakken V, Adamo C, Jaramillo J, Gomperts R, Stratmann RE, Yazyev O,

Austin AJ, Cammi R, Pomelli C, Ochterski JW, Ayala PY, Morokuma K, Voth GA, Salvador P, Dannenberg JJ, Zakrzewski VG, Dapprich S, Daniels AD, Strain MC, Farkas O, Malick DK, Rabuck AD, Raghavachari K, Foresman JB, Ortiz JV, Cui Q, Baboul AG, Clifford S, Cioslowski J, Stefanov BB, Liu G, Liashenko A, Piskorz P, Komaromi I, Martin RL, Fox DJ, Keith T, Al-Laham MA, Peng CY, Nanayakkara A, Challacombe M, Gill PMW, Johnson B, Chen W, Wong MW, Gonzalez C, Pople JA (2003) Gaussian 03, Revision B.04. Gaussian Inc., Pittsburgh, PA
17. Møller C, Plesset MS (1934) Phys Rev 46:618–622
18. Boys SF, Bernardi F (1970) Mol Phys 19:553–566
19. van Duijneveldt FB, van Duijneveldt-van de Ridjt JGCM, van Lenthe JH (1994) Chem Rev 94:1873–1885
20. Simon S, Duran M, Dannenberg JJ (1996) J Chem Phys 105:11024–11031
21. Bader RFW (1990) Atoms in molecules—a quantum theory. International series of monographs on chemistry, no. 22. Oxford University Press, Oxford
22. Bader RFW (1991) Chem Rev 91:893–928
23. Biegler-Koenig FW, Bader RFW, Jang TH (1982) J Comput Chem 3:317–328
24. Ioannou II, Kuczkowski RL (1994) J Phys Chem 98:2231–2235
25. Bone RGA, Bader RFW (1996) J Phys Chem 100:10892–10911
26. Kerkines ISK, Mavridis A (2001) J Phys Chem A 105:1983–1987
27. Kerkines ISK, Mavridis A (2002) J Chem Phys 116:9305–9314
28. Redington RL (1977) J Mol Spectrosc 65:171–189